UDC 669.715:620.178.3.311.5:620.18

STRUCTURAL STATE OF ALUMINUM ALLOY IN VIBRATION LOADING

L. M. Rybakova[1]

Translated from Metallovedenie i Termicheskaya Obrabotka Metallov, No. 4, pp. 24 – 27, April, 2001.

INTRODUCTION

Cyclic loading of structural materials causes more complex processes than single loading. For this reason, despite the numerous experimental data and developed concepts on the fatigue behavior of the material, no unified theory has been created that would allow us to control unambiguously the processes occurring in cyclic deformation and be applicable for practical purposes. Vibration loading has some specific features that complicate the behavior of the material and its fracture still more. The solution of problems of vibration strength requires a study of these features, which is necessary for designing materials capable of withstanding vibration loads. In this connection, we studied the structure of an aluminum alloy and its variation in the process of vibration loading.

METHODS OF STUDY

We chose aluminum alloy of grade AMg-3 for the study. The test specimens (Fig. 1) were cut from a rolled sheet 1.5 mm thick in the direction of the rolling. The specimens were prepared and tested in a vibration stand by the method of a cantilever with one fastened end and one free end at GosNIIAS under the guidance of M. A. Boner. The test regimes and the initial properties of the specimens are presented in Table 1. It should be noted that the difference in the initial values of $\beta_{(331)}$ and *HV* of the specimens is the result of the differences in their preparation and preliminary treatment of the surface.

[1] Institute of Basic Engineering, Moscow, Russia.

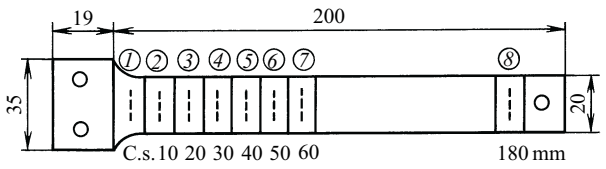

Fig. 1. The pattern of cutting a specimen of alloy AMg-3 after a test on a vibration stand into eight specimens about 10 mm wide (the numbers in the circles correspond to the numbers of the specimens) for x-ray study (C.s. is used to denote the dangerous section).

The study of the fine structure of the specimens was performed with the help of an x-ray method using a sliding ray bundle [1]. The x-ray photographs were taken in cobalt K_α radiation with the ray bundle inclined to the surface by 10°. The specimens for the diffraction analysis tested on the vibration stand were then cut into strips about 10 mm wide by the scheme presented in Fig. 1, where the vertical dashed lines mark the photographed places at various distances from the section critical with respect to the stresses (C.s.). If the specimen did not fail, the region of the first photography coincided with the dangerous section and all the subsequent photographs were taken at distances h = 10, 20, 30, 40, 50, and 60 mm from it. The last photograph was taken at the free end of the specimen at a distance h = 180 mm. For a fractured specimen the first x-ray photograph was taken from the surface layer of the material positioned at a distance of about 1 mm and 3 mm from the edge of the fracture. The subsequent photographs were taken as in the intact specimens at each 10 mm. The obtained diffractograms were used to analyze the interference pattern and its variation over the length of the specimens tested under various conditions of vibration loading. It was established that the width of the x-ray line with the greatest diffraction angle is the most sensitive to changes in the structure. For this reason, we studied in detail the reflection of the x-rays from crystallographic planes (331) (diffraction angle 74°19′). In order to evaluate the width of the interference line its intensity was recorded point by point (photometry) by a MF-4 device. The area F under the curve describing the variation of the intensity of the line was determined by planar geometry. Then we calculated the half-width of the analyzed diffraction line B (in mm) by the formula

$$B = \frac{2}{3}\frac{F}{h}, \qquad (1)$$

where h is the maximum height of the intensity peak.

Due to the low quality of the initial treatment of the specimens and the coarse-grained structure of the aluminum al-

loy and in order to average the experimental data, the photometric curves were obtained under different photometric conditions (the length and width of the slot of the photometer). The value of the true (physical) broadening of the studied x-ray line (β), i.e., with a correction for the constant factor connected with the geometrical parameters of the photography, was determined by the formula

$$\beta = \sqrt{B^2_{(331)} - b^2}, \qquad (2)$$

where $B_{(331)}$ is the value of the full width of the interference line (331) and b is the width of the line connected with the geometrical conditions of the x-ray photography. Under the chosen conditions the geometrical factor $b = 1 \times 10^{-2}$ radian, which is about 1.5 – 2 times less than the width of the line obtained in the derivatogram. The error in the determination of the values of the width of the line was 15 – 20%. However, the great amount of experimental data over the length of the specimen (7 – 9 points) allowed us to determine clear rules of the variation of the width of the line of each specimen after vibration loading of the specimens.

We determined the microhardness in a PMT-3 device under a load $P = 0.5$ N on the indenter. Such a load was chosen for obtaining an indentation 5 – 6 μm deep, which corresponded to the depth of penetration of the ray in the x-ray study. The fluctuations in the values of the microhardness did not exceed 2 – 4% of the mean value for 7 – 10 indentations.

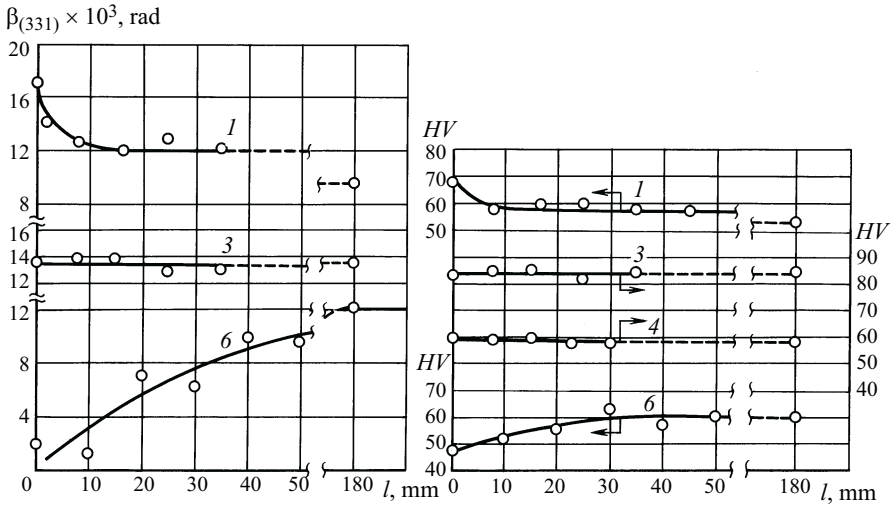

Fig. 2. Variation of the width of the x-ray line $\beta_{(331)}$ and the microhardness HV over the length of specimens of alloy AMg-3 after tests on a vibration stand (the numbers at the curves denote the duration of the tests in h; l is the distance from the fastened end of the specimen).

RESULTS AND THEIR DISCUSSION

Figure 2 presents the results of the measurement of $\beta_{(331)}$ and HV over the length of specimens of alloy AMg-3 tested on a vibration stand for 6 h (without failure). It can be seen that during the first hour of vibration loading the values of $\beta_{(331)}$ and HV increase with the distance from the free end to the fastened end, attaining a maximum in the dangerous section. After 3 and 4 h of testing both the width of the line and the microhardness do not change over the entire length of the specimen including the dangerous section and remain virtually equal to the initial values (before the cyclic loading). The picture changes after 6 h of loading. In the dangerous section and near it the values of the studied parameters decrease substantially (Fig. 2). For greater vividness, we present in Fig. 3 the changes in the width of the line $\Delta\beta_{(331)}$ and the microhardness ΔHV in the dangerous section relative to their initial values after vibration loading of different durations (1, 3, 4, and 6 h). It can be seen that in the process of vibration loading preceding the final failure the material (aluminum alloy in our case) passes through three stages of variation of the physical state. In stage *I* the alloy hardens: during 1 h (100,800 cycles) of vibration loading $\beta_{(331)}$ and HV increase by about 70 and 30%, respectively. In stage *II* this hardening is fully removed. After 3 and 4 h of testing (303,000 and 389,000 cycles, respectively) the studied parameters acquire the initial values ($\Delta\beta_{(331)}$ and ΔHV are virtually zero). In stage *III* after 6 h of testing (561,000 cycles of vibration loading) the aluminum alloy softens: the microhardness and the width of the x-ray line become much lower than the initial values. The value of $\beta_{(331)}$ decreases especially much in the dangerous section (Fig. 2).

The width of the interference line on the x-ray pattern reflects the variation of many parameters of the structure, pri-

TABLE 1. Regimes of Testing Specimens on a Vibration Stand and Initial Characteristics of Aluminum Alloy AMg-3

Specimen	Loading regime		State of specimen	$\beta_{(331)} \times 10^3$, rad	HV
	n	τ, h			
1	100,800	1	Not fractured	9.8	53
2	303,000	3	"	13.6	85
3	389,000	4	"	8.4	57
4	561,000	6	"	12.3	59
5	772,000	8.25	Fractured	7.1	52

Notations: n and τ are the number of cycles and the duration of the loading, respectively; $\beta_{(331)}$ and HV are the width of the x-ray line (331) and the microhardness of the alloy in the initial state, respectively.

Note. All the tests were performed at a vibration frequency $f = 26 – 28$ Hz and amplitude $A = 37.5$ mm. The stress in the control (critical) section of the specimen $\sigma = 135 – 140$ MPa.

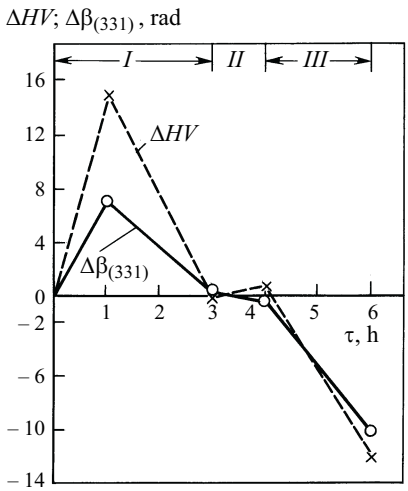

Fig. 3. Change in the variation of the width of the x-ray line $\Delta\beta_{(331)} = \beta^{heat}_{(331)} - \beta^{ini}_{(331)}$ and microhardness $\Delta HV = HV_{heat} - HV_{ini}$ in the dangerous section of specimens after vibration loading of different durations τ: $\beta^{heat}_{(331)}$, HV_{heat} are the characteristics of the alloy after the loading; $\beta^{ini}_{(331)}$ and HV_{ini} are the characteristics in the initial state.

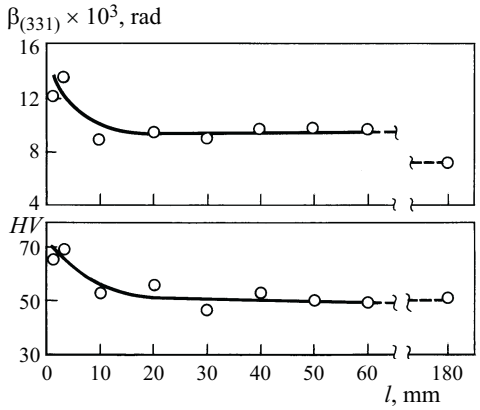

Fig. 4. Variation of the width of the x-ray line $\beta_{(331)}$ and the microhardness *HV* over the length of a specimen tested on the vibration stand until failure (*l* is the distance from the fastened end of the specimen).

marily the degree of defectiveness caused by dislocations, the density of which determines the strength of metals and alloys. The diminished dislocation density and, hence, the softening (reduction of *HV*) in the dangerous section of the aluminum alloy under the action of vibration loads is determined by the special behavior of the structure under sign-variable deformation [2 – 4]. This behavior causes the appearance of point defects in the material (vacancies in particular), the number of which increases with the number of cycles. The vacancies coagulate in the deformation process, forming micropores, and the strength of the material decreases [5]. Maximum stresses in the weakened cross section of the specimen promote nucleation of a microscopic crack, its propagation, and, as a consequence, failure of the specimen. Therefore, it is important to stress that failure of the material in vibration loading is caused by its softening due to the characteristic behavior of the crystal structure in the process of vibration loading. Note that a certain softening of the material (reduction of the microhardness by 7 – 13%) has been observed earlier in studies of the fatigue of some metals [6, 7]. The results presented above show that the softening process is considerably activated by vibration loads; the width of the interference x-ray line decreases by an order of magnitude and the microhardness decreases by more than 30% (Figs. 2 and 3), i.e., the material softens intensely.

We also analyzed the physical state of the aluminum alloy after failure, in our case, in 8 h 25 min or n = 772,000 cycles (see Table 1). In the region of the fracture close to the dangerous section, as well as in the beginning (period *I*) of the vibration loading, the parameters $\beta_{(331)}$ and *HV* increased (Fig. 4). It is known that in cyclic deformation considerable plastic strain appears at the tip of the formed crack and accompanies the development of the crack over the cross section of the specimen until its final failure [8, 9]. The experimental fact (hardening near a fracture) commonly detected after failure allowed many researchers to assume that the nucleation of microcracks under cyclic deformation occurs when the material attains some maximum hardening. However, an analysis of specimens before failure has shown that the cracks appear by another mechanism, i.e., are connected with softening of the material as a result of the intensification of the processes that develop in the crystal structure under vibration loads. In this connection we can suppose that a material (computer designed ones inclusive [10]) serving under vibration loads should be designed from the standpoint of formation of the structural state and its variation in vibration loading, for example, be based on the capacity of the material to damp the processes that cause its softening. Specifically, such is the capacity of the material for aging under cyclic loads [11] that it causes blockage of dislocations and, respectively, suppresses or decelerates the formation of microdefects that cause softening.

CONCLUSIONS

1. We determined the special features of the variation of the structure and microhardness of aluminum alloy AMg-3 in the process of vibration loading under specific test conditions (f = 28 Hz, A = 37.5 mm, σ = 135 MPa).

2. In vibration loading the metallic alloy successively passes through three stages of variation of its physical state: (*I*) hardening; (*II*) softening to the initial level; (*III*) softening below the initial level (maximum softening).

3. Microcracks appear in stage *III*, when the material is in the state of maximum softening. The subsequent propagation of the cracks in the weakened dangerous cross section (due to the softening) leads to final failure of the material.

4. The vibration strength is closely connected with the mechanism of crack formation and the kind of fracture behavior of the material; these factors show that the material should be designed with allowance for the special features of formation of its structure in the process of vibration loading.

REFERENCES

1. L. M. Rybakova, "An x-ray study of the structure of surface layers of plastically deformed metal," *Metalloved. Term. Obrab. Met.*, No. 7, 18 – 20 (1995).
2. A. Cottrell, *Dislocations and Plastic Flow in Crystals* [Russian translation], GosNTI Chern. Tsvet. Met., Moscow (1958).
3. J. Friedel, *Dislocations*, Oxford (1964).
4. B. F. Dem'yanov, E. L. Grakhov, and M. D. Starostenkov, "Interaction between vacancies and special grain boundaries in aluminum," *Fiz. Met. Metalloved.*, **88**(3), 37 – 42 (1999).
5. V. S. Ivanova, *Fatigue Fracture of Metals* [in Russian], GosNTI Chern. Tsvet. Met., Moscow (1963).
6. R. L. Kogan, "A study of a line on a fatigue fracture diagram," *Izv. Akad. Nauk SSSR, Otd. Tekh. Nauk, Metall. Topl.*, No. 3, 78 – 80 (1962).
7. V. I. Belyaev, *A Study of the Fatigue Process in Metals* [in Russian], Izd. Min. Vyssh. Sredn. Obrazov. BSSR, Minsk (1962).
8. N. A. Makhutov, "Fracture diagrams as related to plastic deformations in the crack zone," in: *Problems of Fracture, Service Life, and Safety of Technical Systems* [in Russian], Krasnoyarsk (1997), pp. 93 – 97.
9. I. Zh. Bunin and G. V. Vstovskii, "A physical model of local elastoplastic transformation in fatigue," *Metally*, No. 2, 29 – 40 (1992).
10. V. E. Panin (ed.), *Physical Mesomechanics and Computer Design of Materials* [in Russian], Nauka, Novosibirsk (1995).
11. D. McLean, *Mechanical Properties of Metals* [Russian translation], Metallurgiya, Moscow (1965).